Structure of the B4 Liquid Crystal Phase near a Glass Surface

ARTICLE *in* CHEMPHYSCHEM · JANUARY 2012

Impact Factor: 3.42 · DOI: 10.1002/cphc.201100589 · Source: PubMed

10 AUTHORS, INCLUDING:

Dong Chen
Harvard University
32 PUBLICATIONS **446** CITATIONS
SEE PROFILE

Joseph E. Maclennan
University of Colorado at Boulder
170 PUBLICATIONS **2,934** CITATIONS
SEE PROFILE

Matthew A Glaser
University of Colorado at Boulder
131 PUBLICATIONS **1,505** CITATIONS
SEE PROFILE

David M. Walba
University of Colorado at Boulder
266 PUBLICATIONS **5,318** CITATIONS
SEE PROFILE

DOI: 10.1002/cphc.201100589

Structure of the B4 Liquid Crystal Phase near a Glass Surface

Dong Chen,*[a] Michael-Scott Heberling,[a] Michi Nakata,[a] Loren E. Hough,[a] Joseph E. Maclennan,[a] Matthew A. Glaser,[a] Eva Korblova,[b] David M. Walba,[b] Junji Watanabe,[c] and Noel A. Clark*[a]

The B4 liquid crystal phase of bent-core molecules, a smectic phase of helical nanofilaments, is one of the most complex hierarchical self-assemblies in soft materials. We describe the layer topology of the B4 phase of mesogens in the P-n-OPIMB homologous series near the liquid crystal/glass interface. Freeze-fracture transmission electron microscopy reveals that the twisted layer structure of the bulk is suppressed, the layers instead forming a structure with periodic layer undulations, with the topography depending on the distance from the glass. The surface layer structure is modeled as parabolic focal conic arrays generated by equidistant parabolas whose foci are defect lines along the glass surface. Nucleation and growth of toric focal conics near the glass substrate is also observed. Although the growth of twisted nanofilaments, the usual manifestation of structural chirality in the B4 phase, is suppressed near the surface, the smectic layers are intrinsically chiral, and the helical filaments that form on top of them grow with specific handedness.

1. Introduction

Banana-shaped liquid crystal mesogens with a rigid bent core and one or two flexible tails exhibit a wide variety of novel structural phenomena involving the interplay of chiral, polar, and liquid crystalline order.[1–3] The formation of chiral smectic phases has been a key feature of achiral, banana-shaped molecules, with spontaneous symmetry breaking originally described in the B2 phase of P-9-OPIMB, also known as NOBOW.[4] The first observation of macroscopic chiral domains, however, was in the B4 phase of P-9-OPIMB homologs,[5] where large left- and right-handed chiral domains were distinguished under decrossed polarizer and analyzer. These domains immediately suggested some kind of helical structure[6] and it has since been confirmed that left- and right-handed helical nanofilaments are the structural basis of the B4 phase.[7,8] The bent-core molecules form well-defined smectic layers with in-plane hexatic order, the coupling of macroscopic polarization and tilt of the molecular planes making the layers chiral (Figure 1 a). In this geometry, the half-molecular tilt directions above and below the layer mid-plane are nearly orthogonal (Figure 1 b), so that the projections onto the layer mid-plane of the lattices formed by the core arms do not match and there is a local preference for saddle-splay layer curvature that drives the formation of twisted nanofilaments (Figure 1 c). These nanofilaments are internally crystalline but their mesoscopic organization is liquid crystalline.[7] The existence of helical nanofilaments in the B4 phase has been verified unambiguously by freeze-fracture transmission electron microscopy (FFTEM) images, such as those in Figures 1 d,e. We have proposed that the formation of macroscopic chiral domains of the B4 phase proceeds through the nucleation and chirality-preserving growth of individual helical nanofilaments, with single filaments bifurcating when they exceed a critical width.[8]

Although macroscopic chiral domains have also been observed in the dark conglomerate, a fluid phase of disordered focal conics,[9,10] the B4 is unique in being the only bent-core phase with a macroscopically chiral structure, the twisted filaments. While the dark conglomerate usually appears on cooling directly from the isotropic and changes to crystal at lower temperature,[11–14] the B4 filaments are quite stable and robust, with the properties of the phase preserved even on cooling to room temperature and in mixtures with calamitic LCs (Figure 1 e),[15] making B4 materials of potential use for chiral-optic materials.[16]

Because of their twisted conformation, helical filaments cannot completely fill space near the interface with a flat substrate or make full contact with such a surface. This implies that the structure of the B4 phase must be modified at a liquid

[a] D. Chen,[+] M.-S. Heberling,[+] Dr. M. Nakata,[++] Dr. L. E. Hough, Prof. J. E. Maclennan, Prof. M. A. Glaser, Prof. N. A. Clark
Department of Physics and Liquid Crystal Materials Research Center
University of Colorado, Boulder CO 80309-0390 (USA)
E-mail: Dong.Chen@colorado.edu
Noel.Clark@colorado.edu

[b] Dr. E. Korblova, Prof. D. M. Walba
Department of Chemistry and Biochemistry and
Liquid Crystal Materials Research Center
University of Colorado, Boulder CO 80309-0215 (USA)

[c] Prof. J. Watanabe
Department of Organic and Polymeric Materials
Tokyo Institute of Technology, 2-12-1-S8-42 O-okayama
Meguro-ku Tokyo 152-8552 (Japan)

[+] These authors contributed equally to this work.

[++] Deceased.

Supporting information for this article is available on the WWW under http://dx.doi.org/10.1002/cphc.201100589.

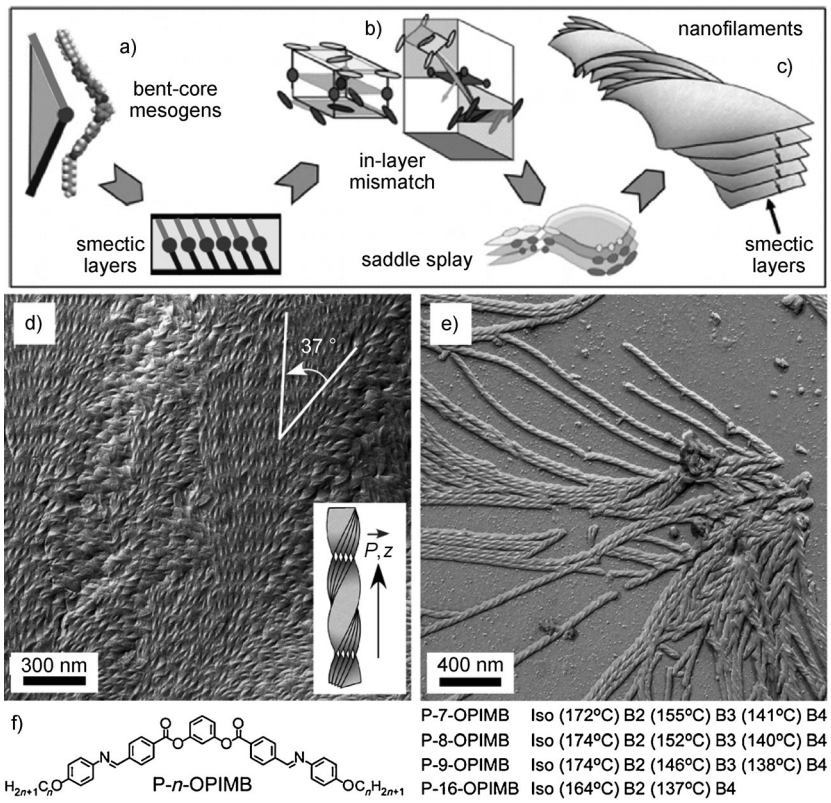

Figure 1. Self-assembly of B4 helical nanofilaments and chemical structures of P-n-OPIMB liquid crystals. a–c) Hierarchical self-assembly of B4 helical nanofilaments. d) Helical nanofilaments of the B4 phase of P-8-OPIMB quenched at room temperature observed by FFTEM. The angle between the helix axis *z* and the helix groove direction is about 37°. e) Helical nanofilaments of the B4 phase of P-9-OPIMB observed by FFTEM in a $c = 75\%$ 8CB/P-9-OPIMB mixture quenched at 37 °C. f) Chemical structures and phase sequences on cooling of the P-n-OPIMB materials investigated.

crystal/glass interface. FFTEM is used here to reveal the surface structure of the B4 phase of bent-core materials in the P-n-OPIMB homologous series, shown in Figure 1 f, and to explore the 3D arrangement of the smectic layers near a liquid crystal/glass interface. Our experiments reveal a rich diversity of surface structures that will help us better understand the complex nature of the B4 bent-core liquid crystal phase.

2. Experimental Section

Freeze-Fracture Transmission Electron Microscopy (FFTEM)

FFTEM experiments are carried out by sandwiching the liquid crystal between 2 mm by 3 mm glass planchettes which are previously cleaned using detergent and then acetone but are otherwise untreated. The planchettes are cooled rapidly from the isotropic to a selected temperature in the B4 range, the phase being confirmed by optical microscopy. The samples are then rapidly quenched to $T < -180\,^{\circ}C$ by immersion in liquid propane, fractured in vacuum at $-140\,^{\circ}C$, and then coated with 2 nm of platinum deposited at 45° and then with 25 nm of carbon deposited at 90°. After dissolving the liquid crystal, the Pt-C replicas are placed in the TEM, where the topographic structure of the fracture plane may be observed. FFTEM images are interpreted on the understanding that regions of the surface facing the platinum shadowing beam appear dark, while those facing away are bright.

3. Results and Discussion

An FFTEM image of P-8-OPIMB fractured near one of the glass planchettes (Figure 2 a) reveals the topography of the B4 phase at different heights above the glass substrate. The upper right part of Figure 2 a shows the typical bulk texture of densely packed B4 helical filaments, growing on top of layer undulation stripes, the B4 surface structure seen in the rest of the image. Unlike the layer undulations observed in the B7 phase, which are a direct consequence of layer thickness variations associated with polarization modulation,[17] or the periodically flattened semi-cylinders observed in thin smectic films frustrated between two interfaces imposing antagonistic anchoring,[18] Figure 2 a shows different topography at different distances from the glass substrate. When the fracture plane is close to the glass (at lower right) we see alternating curved and flat regions, while further away from the glass (at lower left), the surface topography appears as continuous undulations with a periodicity of around 100 nm. The surface structure manifested near the liquid crystal/glass interface can be modeled as a 1D parabolic focal conic (PFC) array of smectic layers. PFCs are a variant of conventional focal conics (if the two foci of an ellipse are infinitely far from each other, the shape of the ellipse near one of the foci approaches a parabola). PFC domains have been observed in many other systems, for example, in dilated smectic A cells[19] and in cholesteric liquid crystal cells with an electric field applied along the twist axis.[20] A 1D PFC array can be constructed from a set of parabolas with their foci along the liquid crystal/glass interface (Figure 2 b). The focus is colinear with the line defect (the structure is translationally invariant along this line) at the interface, which in most cases minimizes the elastic free energy of the system.[18] Due to the fluidity of the B4 phase at high temperature, the line defects can locally anneal into ordered, one-dimensional arrays at the liquid crystal/glass interface. Near the glass (the lower right part of Figure 2 a), the equidistant parabolas are separate and the layers are alternately curved (within the parabolas) and flat (outside the parabolas) as sketched in Figure 2 c. Further from the glass (the lower left part of Figure 2 a), the adjacent parabolas overlap and periodic undulations of the layers are observed, with the layers curving around the line defects within

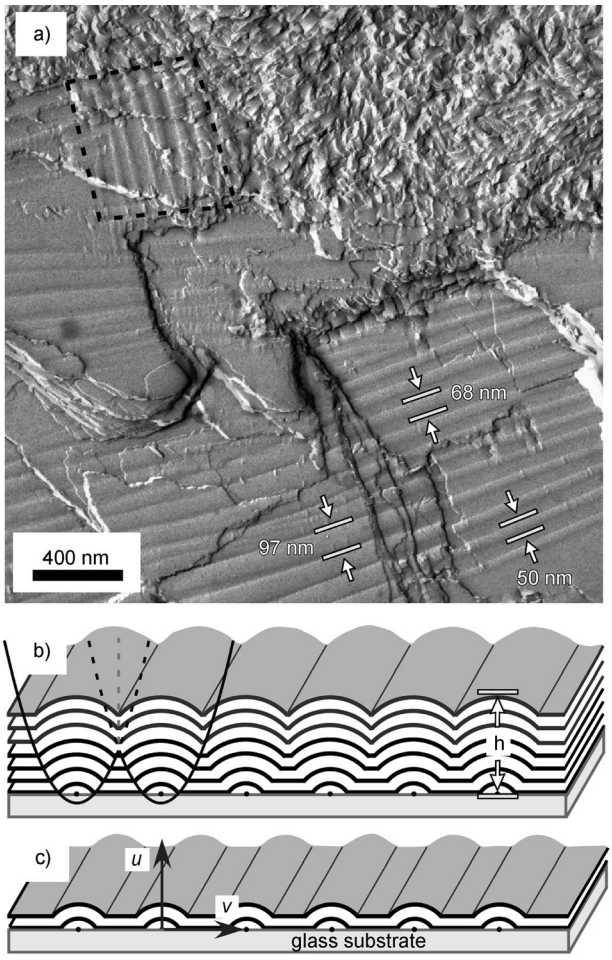

Figure 2. Parabolic focal conic surface structure of the B4 phase of P-8-OPIMB near the liquid crystal/glass interface quenched at room temperature. a) FFTEM image showing the topography of the B4 phase fractured at different heights above the liquid crystal/glass interface. The lower half shows the parabolic focal conic array near the glass, with the lower right closer to the interface and the lower left further away. The region marked at upper left shows a PFC array oriented almost orthogonal to that in the lower half. The rest of the upper half shows the typical self-assembly of helical filaments of the B4 phase in the bulk. b,c) Model of the surface topography of the PFC array fractured at different heights *h*. The curves are parabolas with their foci at the glass substrate. The smectic layers curve around the focus within each parabola and become flat outside, giving alternating curved and flat regions. With each additional layer, the curved regions become wider until the parabolas overlap and the layers show homogeneous, periodic undulations.

the envelope of each parabola as indicated in Figure 2b. By measuring the widths of two undulating regions at different heights, we can compute the form of the parabola. Since the height difference between the regions with 50 and 68 nm periodicity shown in Figure 2a is approximately 10 nm (calculated from the width of the shadowed step between the two regions), the parabola is described by $u-1/(4a)=av^2$ with $a \approx 0.019\ \mathrm{nm}^{-1}$.

Because the glass is essentially untreated, the surface anchoring is very weak, with no clear preference for either homeotropic or planar anchoring of the director. The crucial element inducing the B4 surface structure is thought to be the flat geometry of the substrate, which suppresses the formation of helical nanofilaments at the glass. However, we believe that the in-plane molecular ordering of the PFC array is the same as that in the bulk nanofilaments, for above a certain distance from the glass substrate, helical nanofilaments do appear, growing continuously on top of the undulating layers. The elastic energy density of the PFC is given, to quadratic order of the two principal curvatures σ' and σ'' of the layers, by $f_E = K/2(\sigma'+\sigma'')^2 - \bar{K}(\sigma'\sigma'') + G(\sigma''-\sigma')$, where K and $\bar{K}$ are, respectively, the Frank elastic constants for mean and Gaussian curvature, and G drives curvature in response to the frustrated internal in-plane layer strain β.[7] The minimum of the elastic energy density, shown in Figure S1 of the Supporting Information, is obtained when $\sigma' = -\sigma'' = G/\bar{K}$ (the minimal surface), leading to the adoption of saddle-splay curvature. As the distance from the glass increases, the confining influence of the glass surface on the layers becomes weaker, and the undulating structure of the surface layers eventually transitions to the characteristic bulk helical nanofilament structure, seen in Figure 2a. The PFC surface structure is estimated to penetrate no more than 100 nm into the bulk.

The surface undulations in any given FFTEM image are typically not uniformly aligned along one direction but adopt two degenerate orientations at right angles, as can be seen in Figures 2a and 3a and in Figure S2 of the Supporting Information. This appears to be due to the independent formation of new PFC arrays, which nucleate heterogeneously and grow perpendicular to the edges of existing arrays as shown in the inset of Figure 3a. We have also observed bamboo-like surface structures growing from the boundaries of PFC arrays (shown in Figure 3a) or nucleating independently (shown in Figure 3b and in Figure S3 of the Supporting Information). We propose that this structural variant is made of layers nested in toric focal conic (TFC) domains, with the axial defect line lying at the liquid crystal/glass interface and the circular defect line normal to the glass (see the inset of Figure 3b). A characteristic feature of the bamboo-like structure is that the radial growth is self-limiting, ceasing when the layers extend far away from the axial defect line, as seen in Figure 3b. Similar elastic energy arguments to those limiting the height of the PFC arrays can be applied here. As a smectic layer grows away from the axial defect line, it becomes flatter. Since the layers intrinsically prefer to be curved, this costs more and more elastic energy and eventually the growth terminates. The disordered, fractal-like arrangement of the bamboo-like structure (compared with the ordered PFC arrays) may be a manifestation of quenched disorder, which would occur if they formed at lower temperature and were unable to anneal into ordered arrays. Disordered surface structures with worm-like textures, shown in Figures S4a and S4b (Supporting Information), have also been observed near the glass substrate.

The topology in both the B4 and dark conglomerate phases of bent-core liquid crystals is driven by the tendency for the layers to adopt saddle-splay curvature, which leads to the formation of minimal surfaces that can be realized in the form of helicoid and catenoid. Though the helicoid (Figure S5a, Supporting Information) and catenoid (Figure S5b, Supporting In-

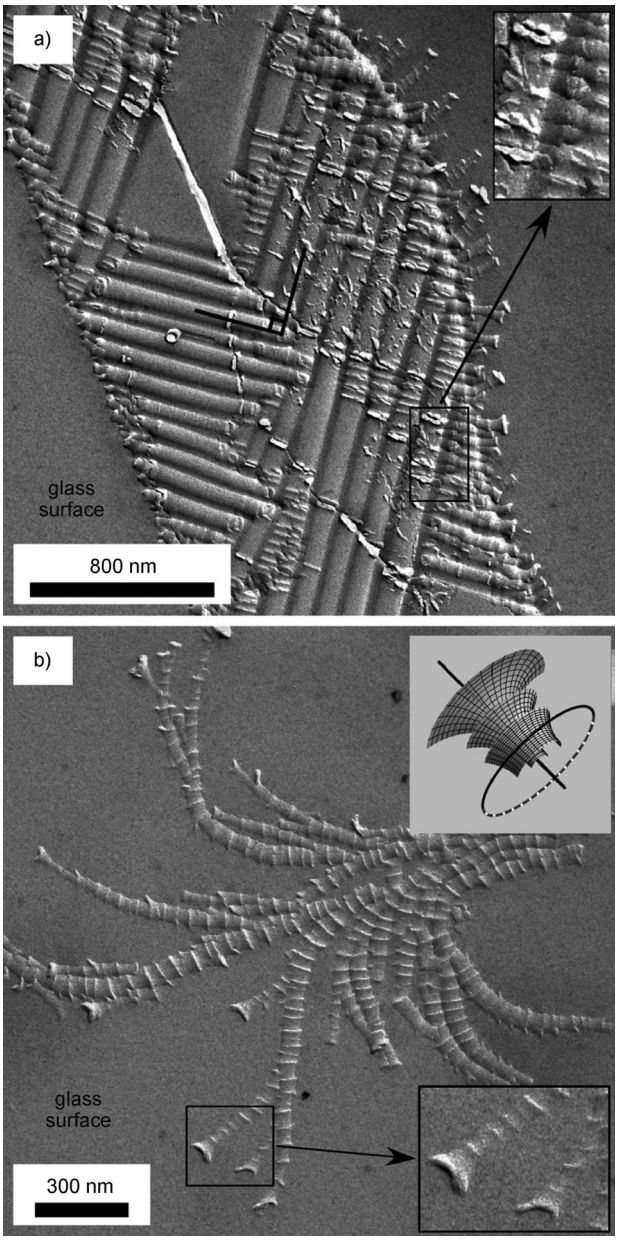

Figure 3. Nucleation and growth of the toric focal conic structure near the liquid crystal/glass interface in the B4 phase of P-7-OPIMB quenched at room temperature and observed by FFTEM. a) Coexistence of parabolic focal conic arrays essentially orthogonal to each other is commonly observed (the smooth regions on either side of the PFC arrays are bare glass). This is a result of the nucleation and growth of new PFC arrays at the edges of existing ones (magnified in the inset). b) Toric focal conics in the B4 phase. This bamboo-like structure, which is also visible along the right boundary of the PFC arrays in a), is made of toric focal conics with their axial defect lines lying along the glass. A model of the layers is shown in the upper inset, with the straight line and the circle representing the line defects. As the layers further from the surface grow, they become flatter (magnified in the lower inset). The reduced curvature raises the elastic energy and inhibits the structure from growing further.

formation) are adjoint structures/topologies, with the same local mean and Gaussian curvatures at equivalent points on the saddle-splay surfaces, the reason why the bulk B4 phase prefers the shape of helicoids, forming helical nanofilaments with structural chirality,[7] while the shape of catenoids dominates in the dark conglomerate phase, with the layers forming disordered focal conics in the bulk[9] or quasi-ordered toric focal conics at the free surface,[10] is still a mystery. The observation of toric focal conics at B4 surfaces (Figure 3b and Figure S6 of the Supporting Information) suggests that focal conics may be thermodynamically close to helical nanofilaments in the B4 phase and might also be observed under the right conditions in bulk B4.

The transition from the B4 surface structure to bulk helical nanofilaments is illustrated in Figure 4a. The filaments appear to be smoothly connected to the underlying PFC arrays, and show characteristic flame-tip-like texture (Figure 4b). The filaments make an angle of about 38° with respect to the PFC stripe direction, essentially matching the angle between the helix axis and the helical groove (~37°, shown in Figure 1d). Careful examination of the filaments in Figure 4b reveals a broken symmetry: the filaments all have the same twist sense (i.e., they are homochiral) and rotate clockwise from the undulation stripes in this case. Although layer twist is suppressed at the glass surface, the smectic layers are nevertheless chiral (the molecules are polar and tilted, as indicated in Figure 4c) and we propose that this chirality is inherited by the helical filaments growing above, leading them to be homochiral and uniformly oriented with respect to the undulation stripes. The projection of the periodicity of the PFC array along the helix axis z of the nanofilaments is about 106 nm (Figure 4b), which is approximately the half-pitch of a filament ($p/2 \approx 108$ nm).[8] The B4 filaments growing on top of the undulating layers thus appear to align their grooves epitaxially along the curved surface layers, as sketched in Figure 4c. This alignment is also observed when nanofilaments grow on the bamboo-like surface structure, as shown in Figure S7 of the Supporting Information.

4. Summary

Freeze-fracture transmission electron microscopy images reveal the diverse topology of the B4 liquid crystal phase near a glass surface. One-dimensional, periodic parabolic focal conic arrays are manifested as smectic layer undulations near the glass. Nucleation and growth of toric focal conic surface structures is also observed. Further from the glass substrate, the layers evolve to the familiar twisted structure of the bulk, with homochiral helical nanofilaments nucleating smoothly on top of the underlying layers and growing epitaxially with the helix groove aligned along the crests of the curved layers. This observation suggests that it may be possible to align B4 helical nanofilaments along one global direction using topographically patterned substrates.

Acknowledgements

The authors are grateful to Ivan Smalyukh for sharing his Mathematica code used to generate focal conic structures. This work was supported by NSF MRSEC Grant DMR-0820579 and NSF Grant DMR-0606528.

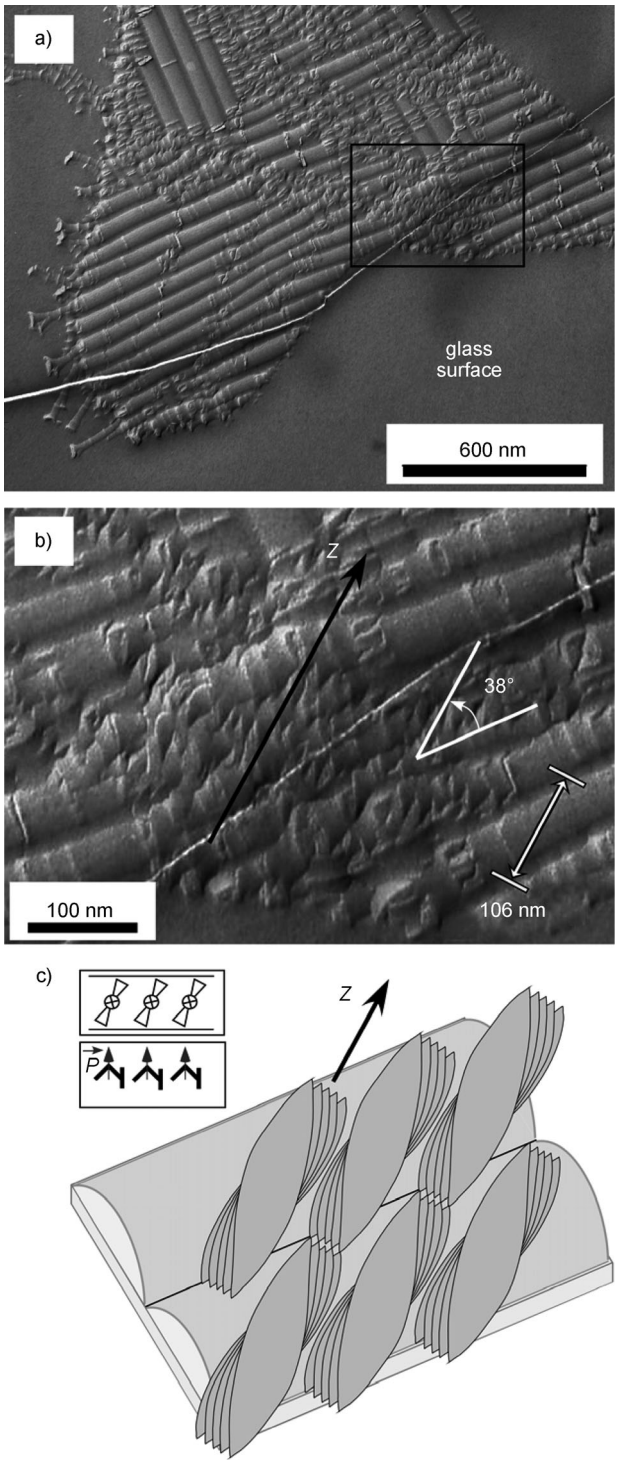

Figure 4. Homochiral helical nanofilaments growing on top of parabolic focal conic surface arrays in the B4 phase of P-7-OPIMB quenched at room temperature. a) FFTEM image showing PFC arrays near the glass and helical nanofilaments above them, as well as bamboo-like toric focal conics at the left boundary. b) Details of the region indicated in (a). Smectic layers forming on top of the undulated surface layers twist into helical nanofilaments. The nanofilaments grow with an orientation of about 38° from the direction of the undulation stripes and have a characteristic flame-tip-like texture. The projection of the periodicity of the PFC array along the helix axis z of the nanofilament is about 106 nm, matching the half-pitch of the filament. c) Cartoon of the transition from undulating surface layers to bulk helical filaments. The inset shows the molecular polarization and molecular tilt which give layer chirality shared in the untwisted surface layers and the twisted nanofilaments.

Keywords: B4 phase · liquid crystals · parabolic focal conic · self-assembly · surface structure

[1] H. Takezoe, Y. Takanishi, *Jpn. J. Appl. Phys.* **2006**, *45*, 597 – 625.
[2] R. A. Reddy, C. Tschierske, *J. Mater. Chem.* **2006**, *16*, 907 – 961.
[3] J. Etxebarria, M. B. Ros, *J. Mater. Chem.* **2008**, *18*, 2919 – 2926.
[4] D. R. Link, G. Natale, R. Shao, J. E. Maclennan, N. A. Clark, E. Körblova, D. M. Walba, *Science* **1997**, *278*, 1924 – 1927.
[5] T. Sekine, T. Niori, J. Watanabe, T. Furukawa, S. W. Choi, H. Takezoe, *J. Mater. Chem.* **1997**, *7*, 1307 – 1309.
[6] J. Thisayukta, H. Takezoe, J. Watanabe, *Jpn. J. Appl. Phys.* **2001**, *40*, 3277 – 3287.
[7] L. E. Hough, H. T. Jung, D. Krüerke, M. S. Heberling, M. Nakata, C. D. Jones, D. Chen, D. R. Link, J. Zasadzinski, G. Heppke, J. P. Rabe, W. Stocker, E. Korblova, D. M. Walba, M. A. Glaser, N. A. Clark, *Science* **2009**, *325*, 456 – 460.
[8] D. Chen, J. E. Maclennan, R. Shao, D. K. Yoon, H. Wang, E. Korblova, D. M. Walba, M. A. Glaser, N. A. Clark, *J. Am. Chem. Soc.* **2011**, *133*, 12 656 – 12 663.
[9] L. E. Hough, M. Spannuth, M. Nakata, D. A. Coleman, C. D. Jones, G. Dantlgraber, C. Tschierske, J. Watanabe, E. Körblova, D. M. Walba, J. E. Maclennan, M. A. Glaser, N. A. Clark, *Science* **2009**, *325*, 452 – 456.
[10] D. Chen, Y. Shen, C. Zhu, L. E. Hough, N. Gimeno, M. A. Glaser, J. E. Maclennan, M. B. Ros, N. A. Clark, *Soft Matter* **2011**, *7*, 1879 – 1883.
[11] G. Heppke, D. D. Parghi, H. Sawade, *Liq. Cryst.* **2000**, *27*, 313 – 320.
[12] J. Thisayukta, Y. Nakayama, S. Kawauchi, H. Takezoe, J. Watanabe, *J. Am. Chem. Soc.* **2000**, *122*, 7441 – 7448.
[13] A. Eremin, S. Diele, G. Pelzl, W. Weissflog, *Phys. Rev. E* **2003**, *67*, 020702/1 – 3.
[14] J. Ortega, C. L. Folcia, J. Etxebarria, N. Gimeno, M. B. Ros, *Phys. Rev. E* **2003**, *68*, 011707/1 – 4.
[15] D. Chen, C. Zhu, R. K. Shoemaker, E. Korblova, D. M. Walba, M. A. Glaser, J. E. Maclennan, N. A. Clark, *Langmuir* **2010**, *26*, 15541 – 15545.
[16] T. Otani, F. Araoka, K. Ishikawa, H. Takezoe, *J. Am. Chem. Soc.* **2009**, *131*, 12 368 – 12 372.
[17] D. A. Coleman, J. Fernsler, N. Chattham, M. Nakata, Y. Takanishi, E. Körblova, D. R. Link, R.-F. Shao, W. G. Jang, J. E. Maclennan, O. Mondainn-Monval, C. Boyer, W. Weissflog, G. Pelzl, L.-C. Chien, J. Zasadzinski, J. Watanabe, D. M. Walba, H. Takezoe, N. A. Clark, *Science* **2003**, *301*, 1204 – 1211.
[18] J.-P. Michel, E. Lacaze, M. Alba, M. de Boissieu, M. Gailhanou, M. Goldmann, *Phys. Rev. E* **2004**, *70*, 011709/1 – 12.
[19] Ch. S. Rosenblatt, R. Pindak, N. A. Clark, R. B. Meyer, *J. Phys.* **1977**, *38*, 1105 – 1115.
[20] B. I. Senyuk, I. I. Smalyukh, O. D. Lavrentovich, *Phys. Rev. E* **2006**, *74*, 011712/1 – 13.

Received: July 29, 2011
Published online on December 8, 2011

